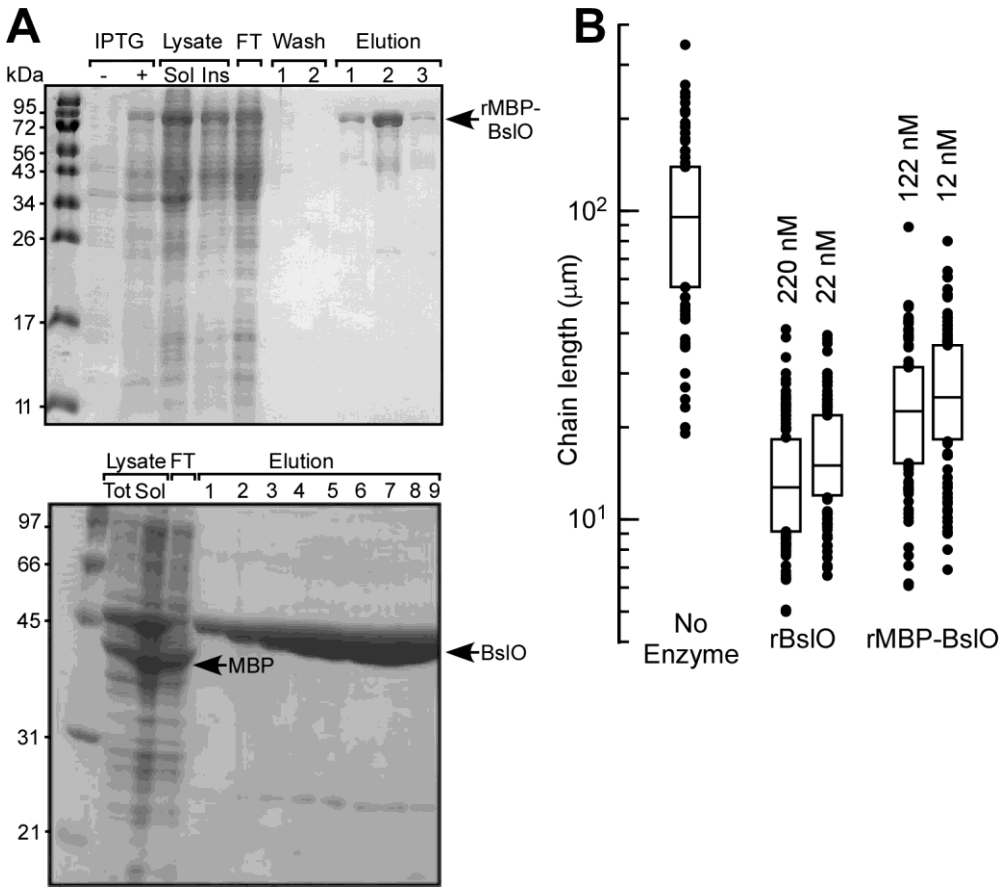


**Figure S1. Purification of MBP-BslO and rBslO from *Escherichia coli*.**

**A.** Upper panel, Coomassie blue-stained SDS-PAGE separating proteins extracted from *E. coli* BL21 (DE3, pMCSG-*bslO*) grown in the absence (-) or in the presence of isopropyl-ß-thiogalactoside inducer (+IPTG). Lysates were centrifuged to separate soluble proteins in the supernatant (Sol) from insoluble proteins in the sediment (Insol). Cleared lysate was subjected to Ni-NTA affinity chromatography, collecting flow-through (FT), column wash (Wash) and eluate fractions (Elution).

Lower panel, Coomassie blue-stained SDS-PAGE separating proteins extracted from *E. coli* BL21 (DE3, pRK1037, pMCSG-*bslO*) grown in presence of isopropyl-ß-thiogalactoside (+IPTG). Constitutive expression of TVMV protease from pRK1037 ensures cleavage of MBP-BslO to generate rBslO. rBslO was purified via Ni-NTA affinity chromatography as described above for MBP-BslO.

**B.** Box and whisker plot of *B. anthracis bslO* mutant chain lengths without or with prior treatment with various concentrations of added rBslO or MBP-BslO. Box bounds $25^{th}$ and $75^{th}$ percentiles. Black bar denotes sample median and black circles represent first and fourth quartile. Data represents 1 of 2 independent biological replicates.

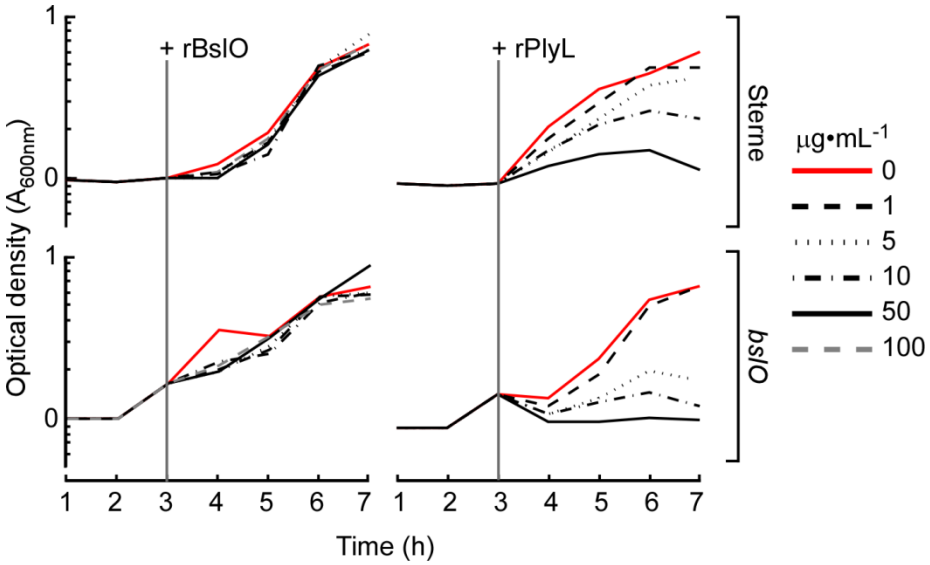


**Figure S2. Growth cultures of *B. anthracis* Sterne or its *bslO* mutant in the presence or absence peptidoglycan hydrolases.**

Growth or lysis of *B. anthracis* vegetative forms was measured as an increase or decrease in absorbance of bacterial cultures at 600 nm light over time, respectively. Time points of addition for purified PlyL or BslO are indicated. Legend denotes the concentration of added PlyL or rBslO.

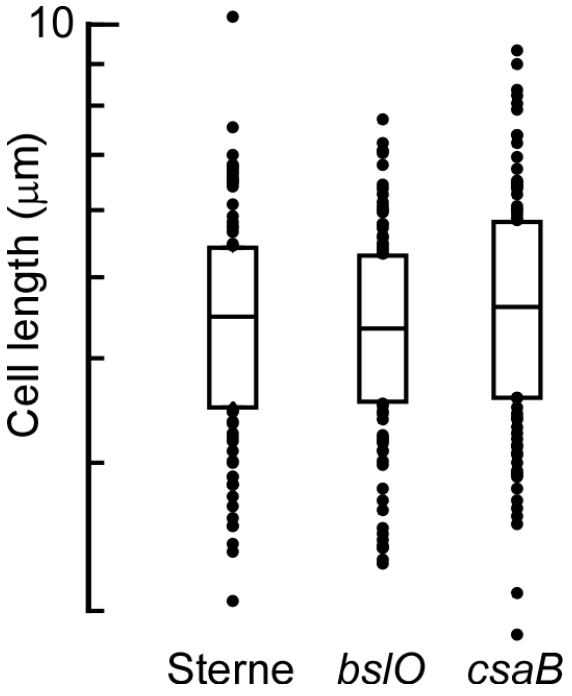


**Figure S3. Cell length of *B. anthracis* Sterne or its *csaB* and *bslO* variants.**

Bacilli were stained with the membrane dye FM4-64 and the distance of membranes adjacent to cell wall septa in *B. anthracis* chains were measured with fluorescence microscopy. Box and whisker plot of cell lengths where the box bounds 25$^{th}$ and 75$^{th}$ percentiles. Black bar denotes sample median and black circles represent first and fourth quartile. N=100 cells examined for each strain. Data represents 1 of 2 independent biological replicates.

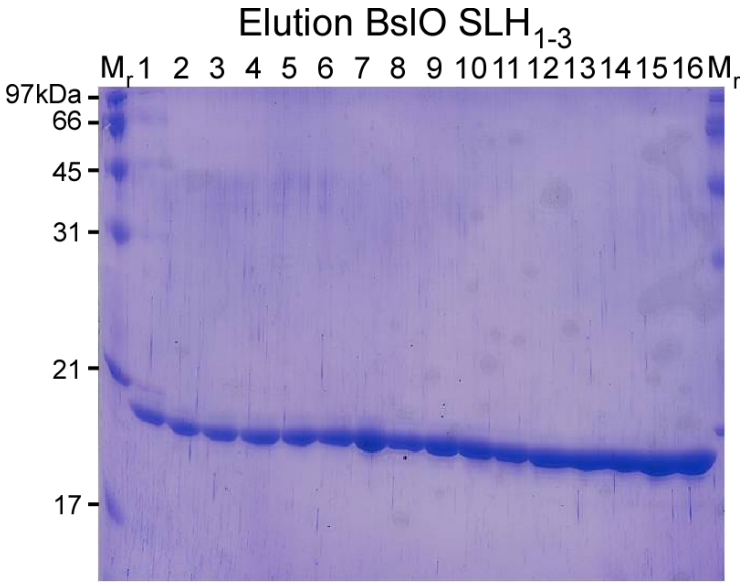


**Figure S4. Purification of BslO-$SLH_{1-3}$ from *Escherichia coli*.**

Coomassie blue-stained SDS-PAGE separating BslO-$SLH_{1-3}$ extracted and purified from *E. coli* BL21 (DE3, p*bslO-SLH*$_{1-3}$). Following rupture of *E. coli* cells in a French pressure cell at 14,000 psi, membranes and insoluble proteins were sedimented by centrifugation, solubilized in Buffer A (6 M guanidine-HCl, 10 mM Tris-HCl, 100 mM $NaH_2PO_4$, pH 8.0) and subjected to Ni-NTA affinity chromatography. The eluate was dialyzed against 50 mM Tris-HCl, 150 mM NaCl, 5% glycerol, subjected to a second round of Ni-NTA purification and collected fractions (1-16) separated on Coomassie-stained SDS-PAGE.

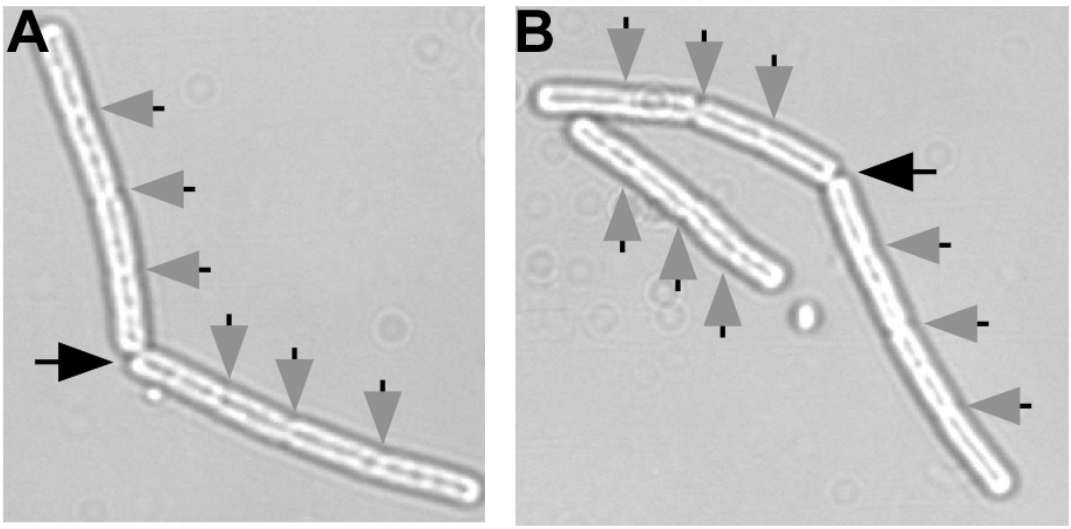


**Figure S5. Septal constrictions in chains of *B. anthracis* Sterne.**

**A, B.** DIC microscopy images of *B. anthracis* Sterne chains reveal varying degrees of constriction at cell wall septa connecting cells within each chain. Deeper invaginations (black arrowhead) occur at septa that are often spaced 4 cells apart, where intermittent septa (grey arrowheads) show either only small or no detectable constrictions.

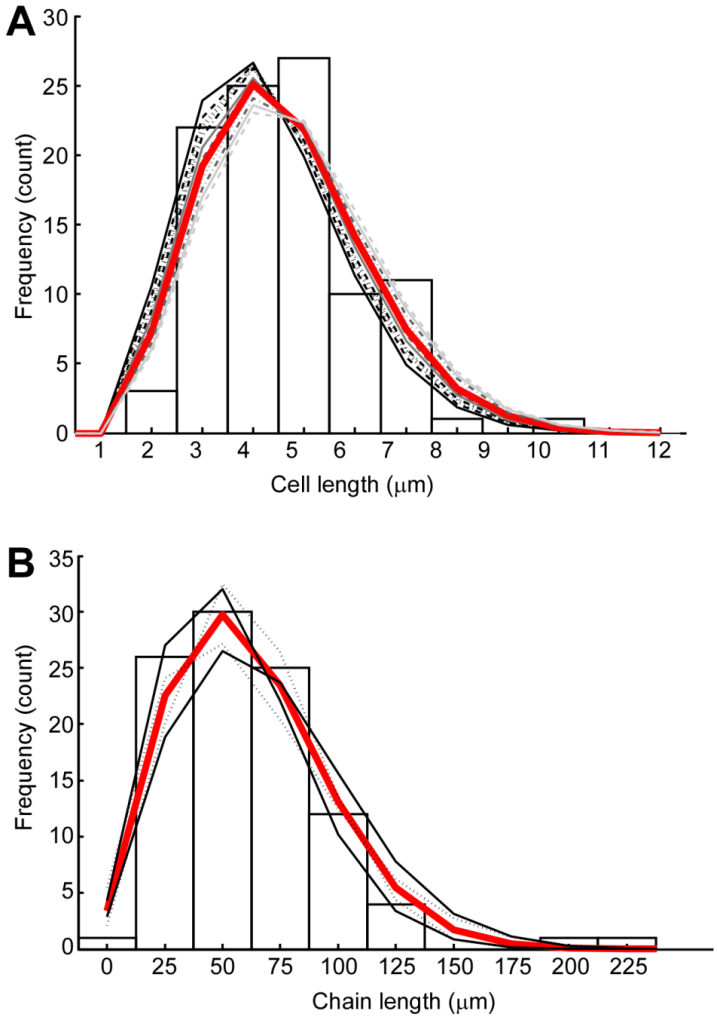


**Figure S6. Simulation of cell and chain lengths of *B. anthracis*.**

Upper panel, simulation of individual cell lengths within *B. anthracis* chains. Histogram (white boxes) represent distribution of experimentally determined individual cell length (N=100). Experimental data was used to estimate λ, the Poisson parameter. Red trace is the mean distribution of 1000 simulations, black and gray traces are the media of 1000 simulations where λ is varied within its 95% confidence interval.

Lower panel, simulation of *B. anthracis* chain lengths using simulated individual cell length data. Histogram (white boxes) represent the distribution of experimentally determined individual chain lengths (N=100). Experimental data were used to estimate the Weibull parameters, *a* and *b*. Red trace is the median distribution of 1000 simulations, black and gray traces bound the 95% confidence intervals of *a* and *b*.

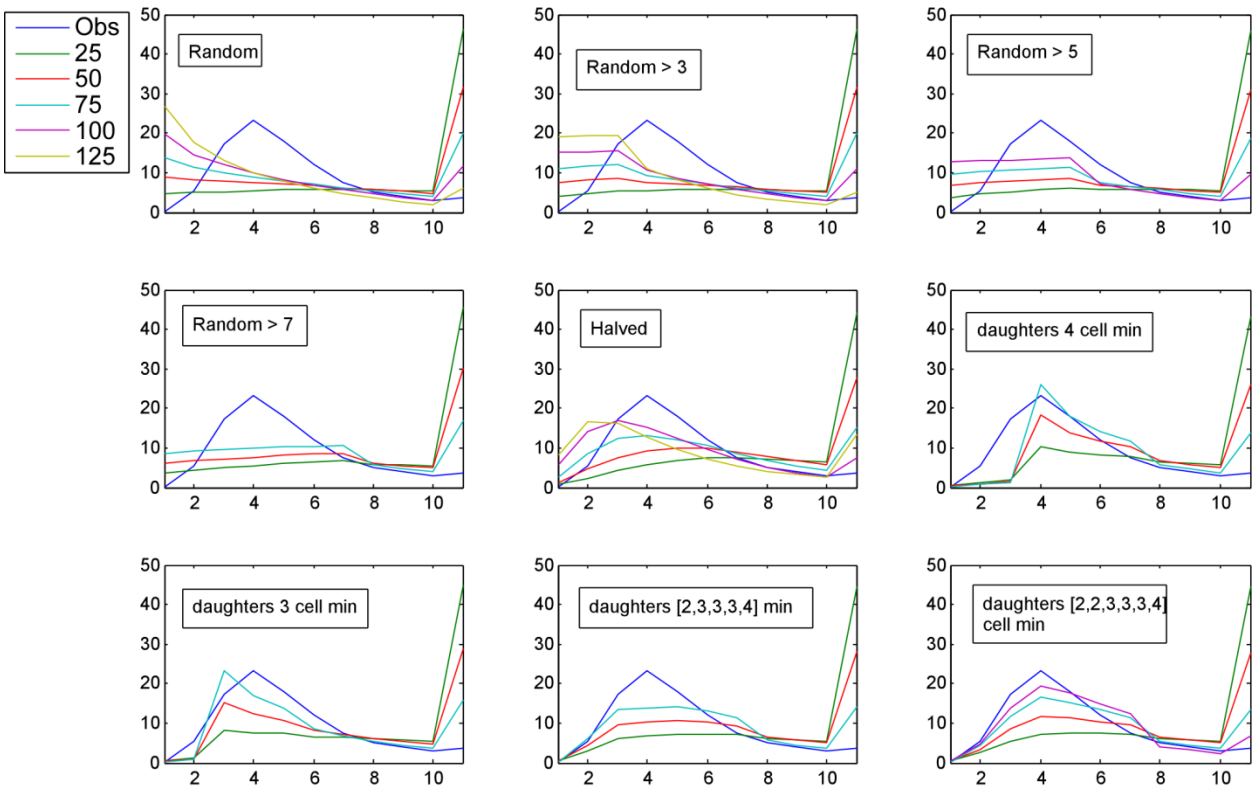


**Figure S7. Modeling *B. anthracis* chain separation.**

Legends identifies observed data (Obs) or the number of allowed septal cleavages in each simulation. Rules impacting the cleavage of *B. anthracis* chains are listed in the insets to each simulation. See text for details.